J Solid State Electrochem (2007) 11:561–570
DOI 10.1007/s10008-006-0195-y

ORIGINAL PAPER

# Electrode kinetics of amperometric hydrogen sensors for hydrogen detection at low parts per million level

**M. Sakthivel · W. Weppner**

Received: 4 April 2006 / Revised: 29 May 2006 / Accepted: 22 June 2006 / Published online: 24 August 2006


**Abstract** Hydrogen gas detection at low parts per million concentration levels in sensors based on polymer membrane electrolytes and catalytically active electrodes, operating at room temperature, is sensitively dependent on the morphology of the electrode. This effect has been investigated using Nafion® as polymeric proton conducting membrane onto which a catalytic electrode was deposited by an *in situ* impregnation-reduction (I-R) technique. In this work, Pt was selected as active catalyst for hydrogen oxidation. The deposition conditions were modified to optimise the parameters with regard to the application of the electrode in low-level hydrogen sensors in the 10–1,000 ppm range and to improve the metal utilisation for reduced electrode loading without loss of electrochemical performance. Models of electrode kinetics are proposed and compared with experimental results. Increasing porosity as a result of decreased reductant concentrations was observed by scanning electron microscopy and other surface characterisation methods. The response time of the hydrogen sensor was in the range of 10–30 s and a stable linear current output was observed under short-circuit conditions.

**Keywords** Hydrogen sensor · Three-phase boundary · Porous electrode · ppm level detection

M. Sakthivel · W. Weppner (✉)
Chair for Sensors and Solid State Ionics, Faculty of Engineering,
Christian Albrechts University,
Kaiserstraße 2,
24143 Kiel, Germany
e-mail: ww@tf.uni-kiel.de

M. Sakthivel
e-mail: msa@tf.uni-kiel.doc

## Introduction

Hydrogen has many potential applications, especially as an energy carrier and especially for combustion in fuel cells, which provide clean, quiet and more efficient energy conversion than other techniques. Hydrogen is also an important raw material in many industrial sectors, such as aerospace, semi-conductor, chemical and food industry. However, handling of hydrogen requires special safety concerns. As hydrogen is explosive above the lower explosive limit (LEL) of 4% in air at room temperature, a sensor is indispensable, which detects traces of hydrogen already in the early stages of leakag. Although different types of sensors are currently known [1–3], most of them show poor response in sensing low hydrogen concentrations in the parts per million (ppm) range. Therefore, the present work is focused on the development of sensor devices with very high sensitivity and selectivity towards hydrogen, especially at or near room temperature.

Polymer electrolytes with high proton conductivities were employed in the present work. The ionically conducting membrane consists of a polymer structure with pendant sulfonic acid groups; a commercially available polymer electrolyte membrane is Nafion® [4]. Such electrolytes with acid group membrane base use widely noble metals such as platinum or noble metal alloys as electrodes [5]. Platinum has excellent electrocatalytic activity for $H_2$ oxidation as compared to other metals [6, 7], high electrical conductivity and high chemical stability in contact with the membrane. However, the electrocatalytic activity of Pt for the $H_2$ redox reaction is critically related to the morphology and geometry of the electrode–electrolyte contact and the three-phase boundary. This is strongly dependent on the particle size and electrode structure. The electrodes must be sufficiently porous to allow the gas to

equilibrate rapidly with the electrolyte and electrode at their interface but not too porous to become a poor electrical conductor. In this paper, an amperometric detector is presented for sensing hydrogen at a Pt | Nafion composite electrode prepared by the chemical reduction method applied subsequently to both sides of the membrane. Surface characterisation techniques such as low-angle X-ray diffraction (XRD), optical microscopy, atomic force microscopy and scanning electron microscopy were used to analyse the chemically reaction-deposited electrodes.

## Theoretical and general considerations

Electrostatic potential drops occur only at the interfaces between the polymer electrolyte and the Pt electrodes in the case of emf measurements as all materials are good electrical (ionic or electronic) conductors. Only for driving electrical currents across the galvanic cell are the commonly small additional electrical fields observed within the electrolyte and across the interfaces (ohmic bulk and interfacial polarisations). The electrostatic potential drops occurring at the interfaces are the result of the equilibration of all mobile charge carriers [8].

Figure 1 shows schematically the chemical potential, electrostatic potential and electrochemical potential of both electrons and protons across the Pt electrode | polymer membrane interface and within the polymer membrane. The fluxes of the protons and electrons by diffusion ($j_D$) are compensated by fluxes in the electrical field ($j_E$) generated by the displacement of the charge carriers, i.e. in the case of ideal behaviour:

$$j_{D,H^+} + j_{E,H^+} = -D_{H^+}\frac{\partial C_{H^+}}{\partial x} - \frac{\sigma_{H^+}}{q}\left(-\frac{\partial \varphi}{\partial x}\right) = 0 \quad (1)$$

$$j_{D,e^-} + j_{E,e^-} = -D_{e^-}\frac{\partial c_{e^-}}{\partial x} - \frac{\sigma_i}{q}\frac{\partial \varphi}{\partial x} = 0 \quad (2)$$

where $D$, $c$, $\sigma$, $q$ and $\varphi$ are the diffusivity, concentration, electrical conductivity, elementary charge and electrostatic potential, respectively.

Considering that the electrical conductivity may be expressed by the product of the concentration and diffusion coefficient [9]

$$\sigma_i = \frac{c_i D_i z_i^2 q^2}{kT} \quad (3)$$

where $z_i$, $k$ and $T$ are the charge number of species $i$, Boltzmann's constant and absolute temperature, respectively, Eqs. 1 and 2 result in

$$\frac{\partial \varphi}{\partial x} = -\frac{kT}{q}\frac{\partial \ln c_{H^+}}{\partial x} = \frac{kT}{q}\frac{\partial \ln c_{e^-}}{\partial x} \quad (4)$$

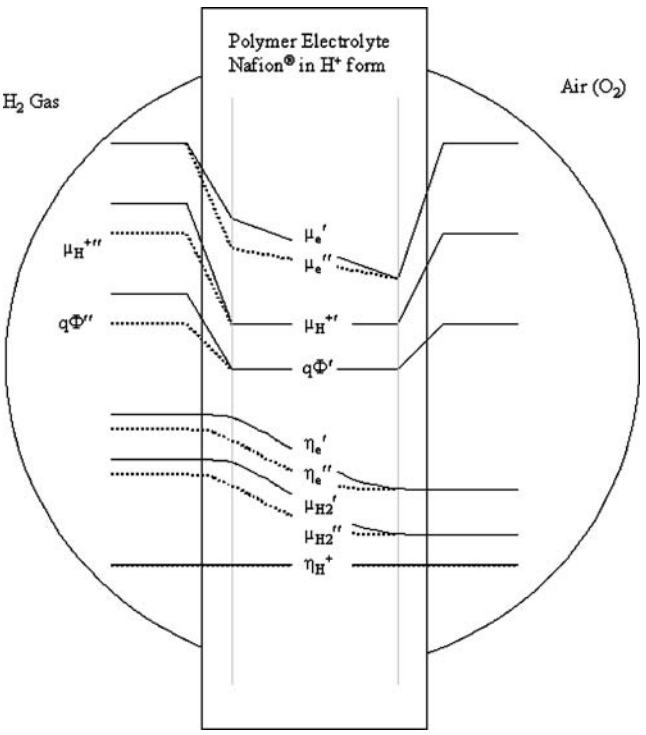


**Fig. 1** Schematic diagram of the chemical potentials of hydrogen, protons and electrons, electrostatic potential and electrochemical potential drop of both electron and proton concentrations along the Pt electrode/polymer membrane interface and within the polymer membrane. *Solid line* represents higher $P_{H2}$; *dotted line* represents lower $P_{H2}$

In the case of non-ideal behaviour, the chemical potential gradient $\partial\mu/\partial x$ has to be considered as driving force, which results in the general formula:

$$\frac{\partial\varphi}{\partial x} = -\frac{1}{q}\frac{\partial\mu_{H^+}}{\partial x} = \frac{1}{q}\frac{\partial\mu_{e^-}}{\partial x} \tag{5}$$

Accordingly, equal magnitudes of chemical potential gradients of protons and electrons are established across the interface. An increased hydrogen concentration in the gas phase results in increased proton and electron concentration in the electrolyte and electrode. This is most noticeable in the phase in which the species are minority charge carriers, i.e. protons in the metallic-conducting Pt and electrons in the proton-conducting electrolyte.

There are two general models of pathways for the protons to reach the electrolyte–electrode interface after they are initially generated from the $H_2$ molecule at the Pt surface exposed to the gas by spending two electrons to the metal electrode. This is schematically shown in Fig. 2.

The dissociative adsorption rate of hydrogen at the platinum surface is determined by the initial sticking coefficient [10] and the probability of molecules/atoms hitting the surface and becoming bound to the surface. The adsorption of hydrogen occurs favourably at Pt surfaces which have a high density of d-electron states, i.e. the sticking coefficient of the (111) Pt surface is close to 1, and there is no energy barrier for the dissociative adsorption of hydrogen [11]. The surface diffusion and the incorporation of hydrogen into Pt are fast. With increasing hydrogen gas partial pressure, the surface area or the number of adsorption sites may eventually become rate limiting for the adsorption of species.

If hydrogen is sufficiently rapidly dissolved and mobile in the platinum, both protons and electrons diffuse to the electrolyte/electrode interface and equilibrium is achieved when the chemical potential of neutral hydrogen is the same at the electrolyte and the platinum electrode side of the interface. It may happen, however, as this is commonly observed for Pt electrodes on oxide ion conductors, that the solubility and transport rate of the mobile ions, i.e. oxide ions, are slow in the bulk of the electrode and the ions

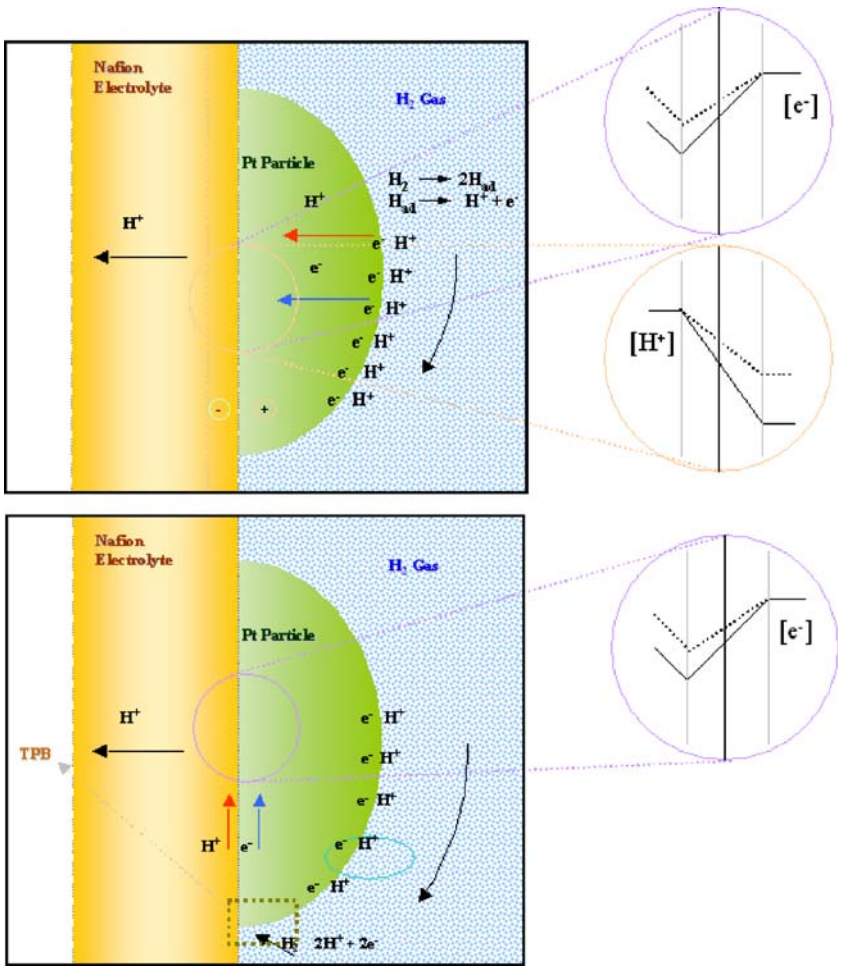


**Fig. 2** Schematic diagram of the process to build up an electrostatic potential drop across the Pt | Nafion interface. The proposed charge diffusion mechanisms are in **a** bulk diffusion and **b** interface diffusion

diffuse along the Pt surface to the electrolyte–electrode–gas triple-phase boundary (TPB). This generates a driving force for the ions and electrons along the electrolyte–electrode interface by chemical diffusion [12]. The electrons may move rapidly in the metallic-conducting Pt while the ions are moving in the electrolyte. The concentration change of the ions results in an equivalent change of the concentration of electrons in the electrolyte and the electrostatic potential drop across the interface will be adjusted accordingly. The galvanic cell voltage is in this case only determined by the equilibration of electrons across the interface. The device may be considered to be a common electronic junction with the only difference that the concentration of the electrons is variable with the outside $H_2$ partial pressure at one side (i.e. in the electrolyte) of the junction. This mechanism was described initially for noble metals in contact with ceramic oxide ion conductors for $O_2$ partial pressure measurements [12].

The equivalent circuit of the diffusional transport mechanism of protons to the Pt–electrolyte interface is shown in Fig. 3. The circuit components $R_{ct}$, $R_b$, $C_I$ and $C_r$ correspond to the resistance of the charge transfer reaction between the Pt electrode (anode) and electrolyte interface, the ionic resistance of the electrolyte, the new double layer capacitances at the left- and right-hand electrode interface upon change of $P_{H2}$ and the capacitance of the double layer at the air reference side (cathode), respectively. The gas diffusion in the electrode may be represented by a Warburg (W) diffusion based on the resistor $R_{ct}$ and capacitor $C_I$.

It is possible that the latter mechanism also holds in the presently employed galvanic cells because of the low operating temperature and the comparatively fast $H^+$ motion along the Pt surface. The chemical diffusion is – in contrast to the bulk of electrolytes – not controlled by the simultaneous motion of slow electrons but by the mobility of the ions in the electrolyte as electrons may move in the metal along the interface for fast compensation of electrical charges.

In the case of electrical currents, the ions are transported through the electrolyte along the cluster network formed by hydrophilic ‘nano-channels’. When the protons reach the opposite cathode–electrolyte interface, a reverse protonic and electronic process occurs, which results in the reaction of the proton with oxygen from air to form $H_2O$ molecules. These water molecules partially diffuse into the electrolyte and maintain the required humidity in the membrane.

Several reports describe processes of metallisation of ionic polymers, i.e. by mechanical, electrochemical and chemical reduction processes [13–18]. An efficient and low-cost method of depositing porous metal electrodes onto the membrane may be achieved by chemical reduction. This chemical deposition process was reported by Takenaka et al. [19], who reduced an anionic metal ion in a solution in contact with one face of the polymer electrolyte membrane by a reductant solution which diffuses through the membrane from a solution in contact with the opposite face. As a variation of this chemical route, the impregnation–reduction procedure was employed by which a cationic metal ion is first impregnated onto the Nafion layer and subsequently reduced [20].

Electrochemical sensor devices are commonly operated either in the current (amperometric) or voltage (potentiometric) measuring mode [21]. The advantage of amperometric gas sensors is a linear relationship between the partial gas pressure and the generated electrical current which can be easily measured with high precision. A wide range of amperometric sensors has been developed for many gaseous compounds [22]. Moreover, amperometry can detect gases in the ppm to percent range with very high precision.

## Experimental aspects

### Membrane pre-treatment

Commercial Nafion membranes, provided by DuPont (Wilmington, DE, USA), were employed in the present work. Nafion membranes are generally characterised by their equivalent weight and thickness. Specifically, Nafion 117 with an equivalent dry weight of the polymer per mol

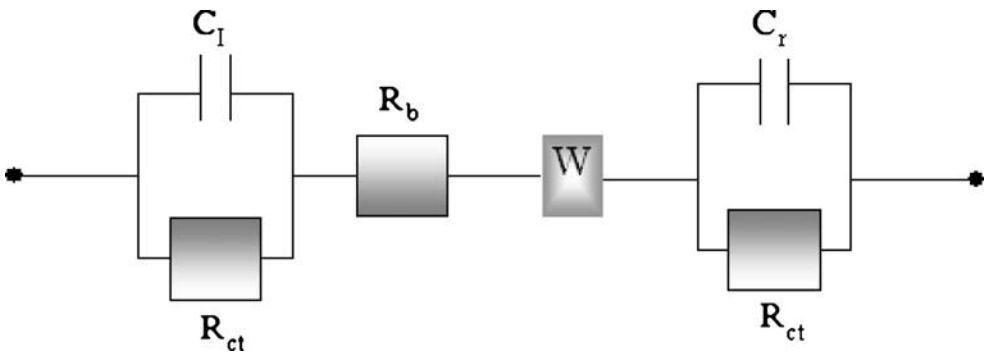


**Fig. 3** Equivalent circuit of a single Pt particle electrode on polymer membrane cell model

sulfonic acid group of 1,100 g/mol which presents a measure for the mass-based concentration of the $SO_3H$ groups and a membrane thickness of 0.7 μm was used. Due to the manufacturing process, as-received Nafion contains sodium ions at some of the exchange sites. Before performing electrochemical measurements, these sodium ions have to be replaced by protons and the membrane has to be swollen in water. This process was performed by boiling the membrane in 3% hydrogen peroxide solution and afterwards in 1 M $H_2SO_4$ for 2 h at a temperature of 100 °C. To remove the remaining acid, the membrane was afterwards boiled three to four times in pure de-ionised water for 30 min. The swollen membranes were stored in distilled water to prevent drying.

### Electrode deposition by chemical reduction and surface characterisation

The ionic polymer–metal electrodes were prepared by chemical treatment of the ionic polymer by employing the impregnation–reduction method [23] with an ionic salt solution of a metal complex such as tetra-ammine platinum (II) chloride $[Pt(NH_3)_4Cl_2{\cdot}H_2O]$ purchased from Sigma Aldrich in 0.001, 0.01 and 0.1 M concentrations. The membrane was stretched and fixed in a polyacrylic holder with a circular opening of 16 mm in diameter. The metal complex solution was exposed to the membrane for 3 h at a fixed pH value of 11–12 maintained by the addition of ammonium hydroxide solution. This addition of $NH_4OH$ to the platinum complex solution enriches the cationic metal ions. Those metal ions are easily exchanged in a protonated polymer chain network. Then, the membrane was rinsed two to three times with double-distilled water to remove the excess of the platinum complex solution from the membrane. The impregnated metal ions $[Pt(NH_3)_4]^{2+}$ were reduced by using a weak reducing agent, i.e. potassium tetrahydroborate ($KBH_4$), with 0.006, 0.008, 0.01, 0.02 and 0.04 M concentrations for 2 h. The reducing solution was replaced every 20 min. Both impregnation and reduction were carried out at room temperature. A similar procedure was subsequently applied to the other side of the membrane to prepare the counter electrode with the same thickness as the opposite one. Different sets of samples were prepared and became marked as sample KB *m x* (*m* represents the molar reductant concentration and *x* describes various samples of the same set by using subsequent letters, i.e., a, b, c, etc.). All chemically reduced ionic polymer–metal surfaces were examined by a high-resolution optical microscope (LEICA MZ26), a scanning electron microscope (Philips XL30) and an X-ray diffractometer (Seifert XRD 3000). Further experimental details are described in detail elsewhere [24].

## Hydrogen gas measurements

The schematic drawing of the assembled hydrogen sensor cell is shown in Fig. 4. Sensor testing was performed at ambient pressure and room temperature with a common moisture of 50–60% relative humidity (RH) at a gas flow

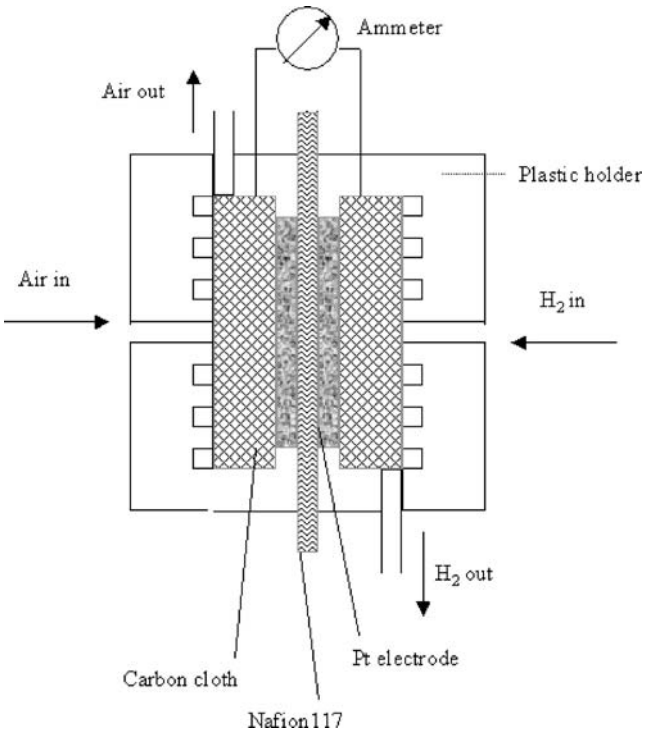


**Fig. 4** Schematic diagram of the ionic polymer–metal component sandwiched between Plexiglas compartments

rate of 80 sccm. High-purity dry hydrogen and hydrogen–nitrogen gas mixtures (Messer-Griesheim, Germany), containing 1 and 10% hydrogen partial pressures, were used for the investigations. The parent gases from the gas cylinders were diluted by mixing with $N_2$ in various ratios down to the ppm level using commercial mass flow controllers (EL-Flow mass flow meter/controller, Bronkhorst, Ak Ruurlo, Netherlands). The hydrogen gas response of the cell was analysed by using an Ionic Systems potentiostat/galvanostat PG2 (Stuttgart, Germany). Gas exposure times were typically 60 s or as specified in the figure captions, during which the sensor signal usually reached a steady-state value. The sensitivities are given by the slope of the calibration curve ($\mu A\ ppm^{-1}$) and the response time $t_{90}$ is given by the time to reach 90% of the change of the steady-state signal.

## Results and discussion

### Bulk and surface characterisation of the electrode

The crystal structure and the particle size were both analysed by means of XRD. Figure 5 shows the X-ray diffraction patterns of the platinum electrode samples deposited by applying 0.01 M $Pt(NH_3)_4Cl_2$ metal salt solution and five different concentrations of reducing agent, i.e. 0.006, 0.008, 0.01, 0.02 and 0.04 M $KBH_4$ (from top to bottom). The vertical line pattern shows the data of the standard JCPDS card 4-802 [25]. All peaks could be well indexed according to the standard. All five XRD patterns show only Pt peak angles, irrespective of the concentration of the reducing agent, i.e., the $[Pt(NH_3)_4]^{2+}$ ions of the impregnated Nafion membrane were reduced completely. The peaks observed for lower concentrations of the reducing agent show larger distortions than that observed for higher concentrations as well as larger broadening, which is attributed to induced strain between the Pt particles. Smaller particle sizes are expected in the case of broader peaks. The size of the Pt particles was calculated using Scherrer's equation [26], evaluating the full width at half maximum of the peak broadening by using the peakfit program (http://www.clecom.co.uk/science/peakfit/index.html). The instrumental broadening is subtracted, using the expressions as described elsewhere [27].

Optical microscope images of the chemically reduced platinum electrode surfaces have shown different surface morphologies for the five reductant concentrations of 0.006, 0.008, 0.01, 0.02 and 0.04 M $KBH_4$. Micrograph images show Pt surfaces of less strain and porous structures unlike those observed in the case of $NaBH_4$ reductant [28].

Scanning electron microscope (SEM) images of the porous structures of the chemically reduced ionic polymer–platinum electrode surfaces are shown in Fig. 6. Pt deposited at the lowest (0.006 M) $KBH_4$ concentration resulted in isolated and inhomogeneous platinum particles deposited on the Nafion membrane. This phenomenon can be understood by considering insufficient reduction time at low reductant concentration to reduce all $[Pt(NH_3)_4]^{2+}$ ions. The Pt surface of the sample prepared with 0.04 M $KBH_4$ shows high strain and an increased particle size. In addition, both sample surfaces show a large variation in porosity. The samples prepared with an intermediate 0.01 M concentration of $KBH_4$ as reducing agent provide more homoge-

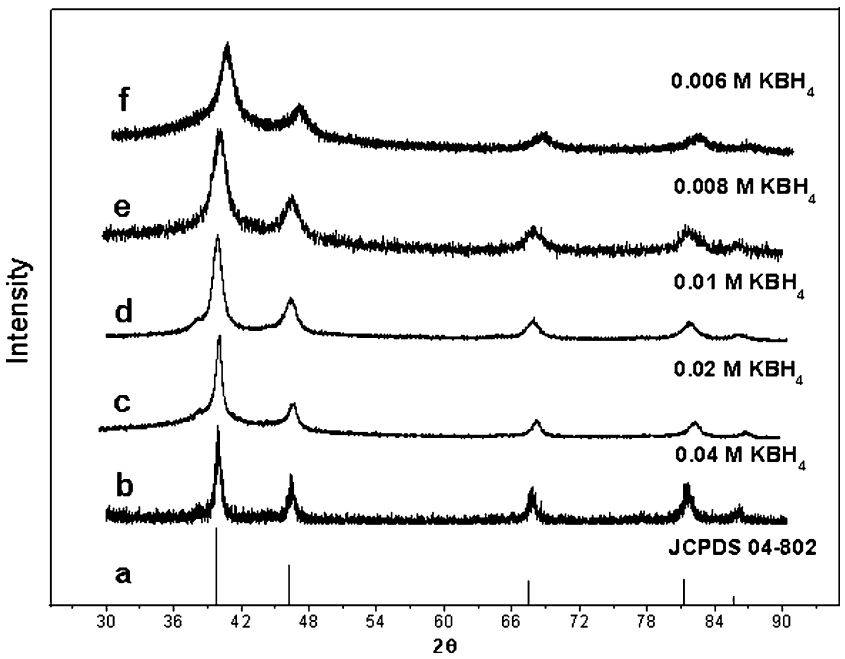


**Fig. 5** X-ray diffraction pattern of Pt | Nafion electrode prepared from 0.01 M Pt $(NH_3)_4Cl_2$ and five different reductant concentrations: **a** JCPDS 04-802, **b** 0.04 M, **c** 0.02 M, **d** 0.01 M, **e** 0.008 M and **f** 0.006 M $KBH_4$

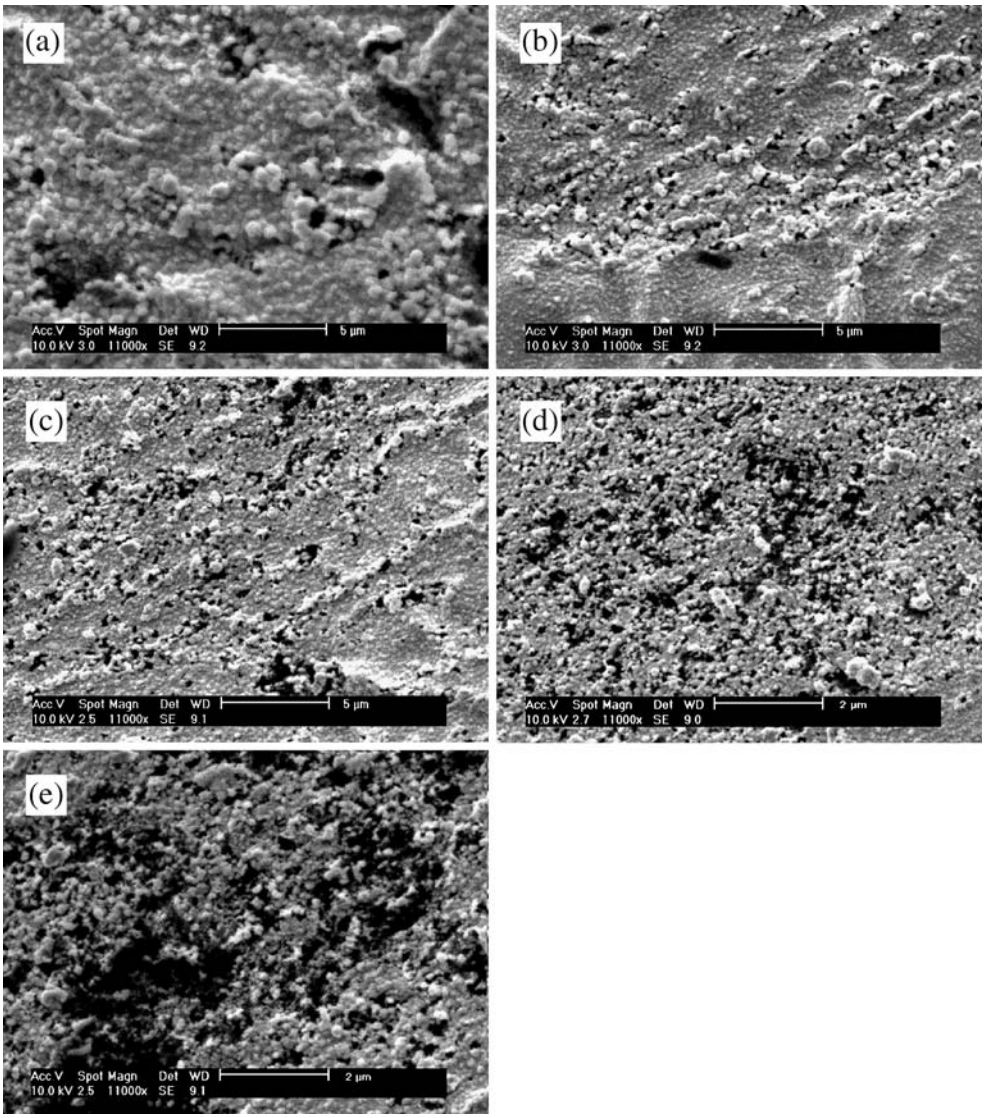


**Fig. 6** SEM photograph of Pt electrode deposited on Nafion117 membrane using 0.01 M $Pt(NH_3)_4Cl_2$ and reductant concentrations: **a** 0.04 M, **b** 0.02 M, **c** 0.01 M, **d** 0.008 M and **e** 0.006 M $KBH_4$

neous pores than in the case of 0.02 and 0.008 M. Porous structures were obtained due to the weak reducing nature of the $KBH_4$. Similar conditions were applied when five Pt electrodes were prepared using five different $NaBH_4$ concentrations with different reduction rates. The higher the reduction rate, the more strain and particle growth is observed. Lower reductant concentrations show less strain and slow growth rate, resulting in poor interparticle contact.

The SEM images of the Pt particles deposited onto the Nafion membrane show different crystallite sizes, which are in agreement with the sizes calculated from XRD peak analysis. The SEM investigations confirmed the tendency of decrease in particle size and increase in porosity with increasing reductant concentration. Energy dispersive X-ray spot analysis shows Pt peaks in the M and L energy levels and a small percentage of fluorine and carbon peaks due to the base perfluorated polymer membrane. The images of the surfaces observed for the highest reductant concentration show thick layers of Pt fully covering the electrolyte surface. This coverage is less suitable for sensor applications, in which the three-phase boundary region is of primary importance.

## Electrode kinetics

By assuming that the Pt particles are semi-spherical in shape and homogeneous in size, the radius of the particles is equal to the diffusion length $L$ of the protons, and it may be related to the response time according to:

$$\tau = \frac{L^2}{2D_{H^+}} \tag{6}$$

According to Fig. 2, based on model 1, the response time $\tau_1$ of proton diffusion through the Pt particle is 5 s by considering that the diffusion coefficient of the protons $D_{H+}$ in Pt is $10^{-9}$ $cm^2/s$ [29]. In contrast, based on model 2, $D_{H+}$ in Nafion at 27 °C is $10^{-6}$ $cm^2/s$ [30]; thus, the response time $\tau_2$

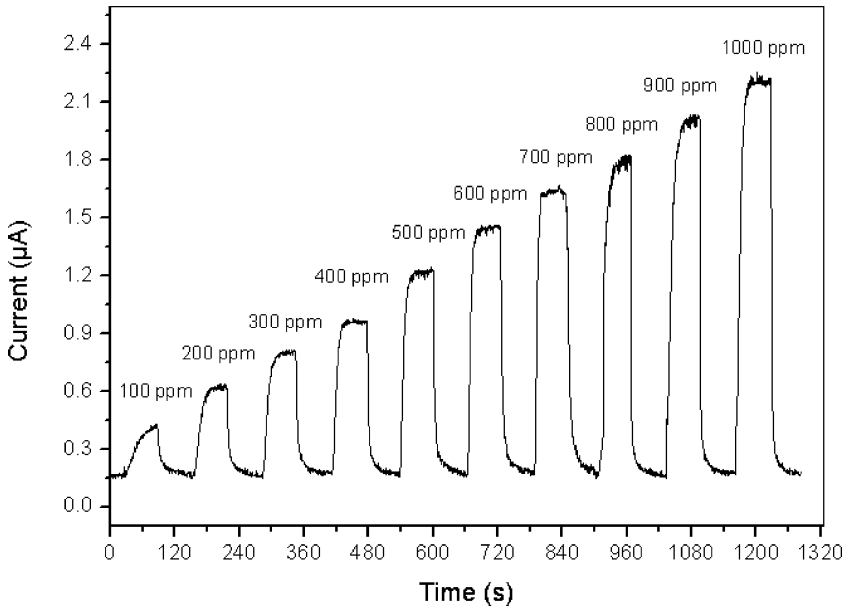


**Fig. 7** Response behaviour of the Pt | Nafion electrode sensor element with an area of 2 $cm^2$ prepared from 0.01 M Pt $(NH_3)_4Cl_2$ and 0.01 M $KBH_4$ (sample KB1a) for hydrogen gas in the low concentration range of 100–1,000 ppm

of proton diffusion along the electrode/membrane interface is 5 ms. According to Eq. 3, the calculated $D_{H+}$ in Nafion at 27 °C is $10^{-7}$ $cm^2/s$ for 1 M $H_2SO_4$ concentration and the proton conductivity in Nafion is $10^{-2}$ S $cm^{-2}$. There is one order of magnitude difference which may be due to the presence of fluorine groups in the membrane which has not been taken into account. As the response time $\tau_2$ is three orders of magnitude faster than what is expected from model 1, it may be assumed that the diffusion of hydrogen along the surface of Pt is faster than the diffusion of hydrogen along the Pt electrode/polymer membrane interface. The surface of Pt is always covered with hydrogen gas and the gas may supply a sufficient amount of hydrogen which is consumed at the triple-phase boundary. Thus, the concentration of hydrogen species arriving at the Pt electrode/polymer membrane interface for the charge transfer reaction is related to the surface diffusion rates and surface coverage [31].

## High hydrogen gas concentration response

Optical micrographs of the Pt electrode surfaces prepared with 0.006–0.04 M $KBH_4$ have shown higher porosity. The typical responses of the interface Pt electrode | Nafion (0.01 M $Pt(NH_3)_4Cl_2$ and 0.01 M $KBH_4$) (sample KB 1a) to various concentration steps in the 100–1,000 ppm range of hydrogen in nitrogen at room temperature are given in Fig. 7. A plot of (sample KB1a–d) the maximum output current of the sensor vs the hydrogen gas concentration is linear as shown in Fig. 8. The correlation coefficient $R$ of the linear regression is 0.9995. The average maximum sensitivity of the sensor is 2.6 nA $cm^{-2}$ $ppm^{-1}$. Between 100 and 1,000 ppm hydrogen, the response time $t_{90}$ is in the order of 25 and 5 s in the direction of increasing and decreasing $H_2$ concentration, respectively.

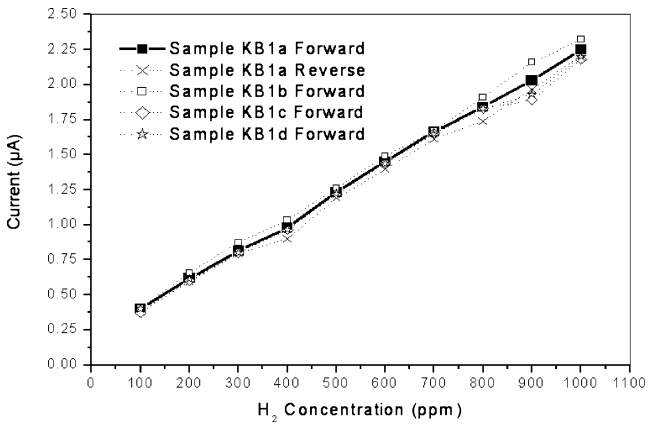


**Fig. 8** Linear relation for 0.01 M $KBH_4$ (sample KB1a) concentration over a wide range of hydrogen concentration (100–1,000 ppm) and a sensing area of 2 $cm^2$. The *dotted lines* are results from calibrations with different samples

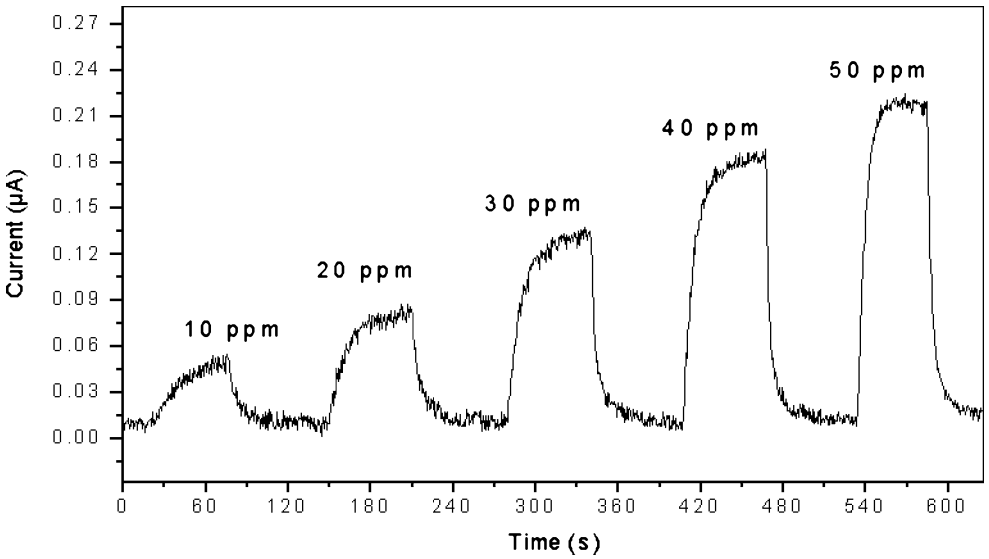


**Fig. 9** Response behaviour of the Pt | Nafion electrode sensor element with an area of 2 $cm^2$ prepared from 0.01 M Pt $(NH_3)_4Cl_2$ and 0.01 M $KBH_4$ (sample KB1a) for hydrogen gas in the low concentration range of 10–50 ppm

## Low hydrogen gas concentration response

The same set of samples was exposed to 10–50 ppm hydrogen. The response curve for 1 min exposure to 10–50 ppm $H_2$ is shown in Fig. 9. Linear output current responses were observed for different samples over this hydrogen concentration range as presented in Fig. 10. The correlation coefficient $R$ of the linear regression is 0.99746. The average maximum sensitivity of the sensor is 4.6 nA $cm^{-2}$ $ppm^{-1}$.

The linear behaviour for all concentrations of the reducing agent can be explained by the achievement of highly effective electrodes by the formation of porous structures. The optimum porous structure obtained for 0.01 M $KBH_4$ was most favourable for detection at a very low concentration level.

The thicknesses of the electrodes were determined by surface profilometry, which depends on the concentrations of

**Table 1** Electrode characterisations and hydrogen sensitivities of the Pt Nafion electrodes

| Metal salt concentration (mol) | Reductant concentration (mol) | Electrode thickness (μm) | $H_2$ sensitivity (10 ppm) (μA) |
|---|---|---|---|
| 0.001 | 0.04 | 0.36 | 0.012 |
| 0.1 | 0.04 | 2.10 | 0.030 |
| 0.01 | 0.006 | 0.15 | – |
| 0.01 | 0.008 | 0.20 | 0.023 |
| 0.01 | 0.01 | 0.30 | 0.050 |
| 0.01 | 0.02 | 0.46 | 0.031 |
| 0.01 | 0.04 | 0.62 | 0.008 |

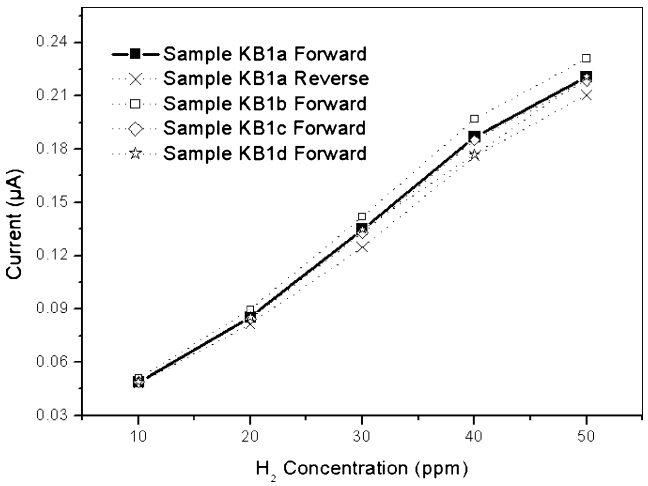


**Fig. 10** Linear relation for 0.01 M $KBH_4$ (sample KB1a) concentration over a low level of hydrogen concentration (10–50 ppm) and a sensing area of 2 $cm^2$. The *dotted lines* are results from calibrations with different samples

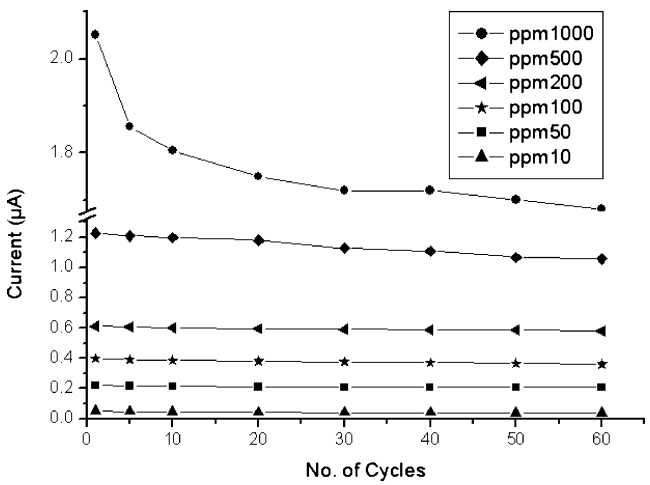


**Fig. 11** Stability of the sensor element Pt Nafion with an electrode of an area of 2 $cm^2$ and prepared from 0.01 M $Pt(NH_3)_4Cl_2$ and 0.01 M $KBH_4$ for different hydrogen gas concentrations up to 60 cycles

the reducing agent being used. The electrodes prepared with different concentrations of both Pt metal salt and reductant deposited in various electrode thicknesses and their sensitivity to 10 ppm $H_2$ are listed in Table 1. Even though the electrode thickness increases by varying the reductant concentration, the maximum sensitivity was obtained for the 0.01 M $KBH_4$ sample. The responses of the other samples were observed to be nonlinear in the low hydrogen partial pressure range. The amount of large pores increases the gas diffusion in the electrode although the increase was not large enough to produce sufficient electronic interparticle contact.

Figure 11 shows a number of identical cycles that attained the maximum output current measured for 10–1,000 ppm of hydrogen gas concentrations. The typical hydrogen responses for multicyclic gas exposure of the sensor were observed for each concentration. The response time ($t_{90}$) was typically less than 10–30 s. Figure 11 shows that the sensor remains stable over a large number of cycles. It should be pointed out that with increasing hydrogen concentration, when the hydrogen level is above 1000 ppm, the amount of water and heat generated by the reactions of the sensor increases simultaneously. Hence, the conductivity of Nafion and the temperature of the sensor are increased, which likely causes the nonlinearity of the observed response current. Up to 400 ppm, the maximum current was constant over several cycles, but in the higher concentration range the current was observed to decrease after 15 cycles. A downward drift was observed to be due to water becoming electrochemically generated at high hydrogen concentrations which is firmly held within the structure of the hydrophilic Nafion. Furthermore, the process leading to the attainment of an equilibrium water content corresponding to a given RH of the test gas is slow. The lower detection limit for $H_2$ was 10 ppm, below which the current signal was highly unstable.

## Conclusions

The structure and gas sensing performance of a practically applicable short-circuited amperometric sensor composed of a chemically reduced catalytic Pt electrode and solid polymer membrane was demonstrated. The Pt electrodes prepared with 0.01 M $KBH_4$ reducing agents showed a stable and linear response to hydrogen gas in the 10 to 1,000 ppm range. The charge transfer reaction is related to the surface diffusion rates of hydrogen along the Pt surface and the surface coverage. Among the proposed two models, the latter one is likely consistent with the experimental results. The sensor measurement results show a clear tendency of fast response rate with increasing amounts of porosity in the electrode. Small pore size structures provide shorter diffusion lengths of the proton to and along the Pt | Nafion interface. A combination of high active surface areas and porous electrodes allows the application of the device in the 10–1,000 ppm range of hydrogen gas detection at room temperature.

## References


1. Bouchet R, Rosini S, Vitter G, Siebert E (2001) Sens Actuators B 76:610
2. Favier F, Walter EC, Zach MP, Benter T, Penner RM (2001) Science 293:2227
3. Baselt DR, Fruhberger B, Klaassen E, Cemalovic S, Britton CL, Patel SV, Mlsna TE, McCorkleand D, Warmack B (2003) Sens Actuators B 88:120
4. Hamnett A (1996) Fuel cells and their development. Philos Trans R Soc Lond Ser A 354:1653–1669
5. Gottesfeld S, Zawodzinski TA (1997) Polymer electrolyte fuel cells. In: Alkire RC, Gerischer H, Kolb DM, Tobias CW (eds) Advances in electrochemical science and engineering. Wiley-VCH, Weinheim, pp 195–231
6. Setoguchi T, Okamoto K, Eguchi K, Arai H (1992) J Electrochem Soc 139:2875
7. Jiang SP, Badwal SPS (1997) J Electrochem Soc 144:3777
8. Weppner W (2003) Ionics 9:444
9. Rickert H (1982) Electrochemistry of solids. Springer, Berlin Heidelberg New York, pp 78–86
10. Christmann K (1988) Surf Sci Rep 9:1
11. Frumkin AN (1963) In: Delahay P, Tobias CW (eds) Advances in electrochemistry and electrochemical engineering, vol. 3. Wiley-Interscience, NY, pp 287–391
12. Tsagaraki ED, Weppner W (2001) Proceedings—Electrochemical Society (solid-state ionic devices II: ceramic sensors) 2000-32:285
13. Jeong HM, Woo SM, Lee S, Cha GC, Mun MS (2006) J Appl Polym Sci 99(4):1732
14. Deronzier A, Moutet JC (1998) Platin Met Rev 42(2):60
15. Centomo P, Zecca M, Lora S, Vitulli G, Caporusso AM, Tropeano ML, Milone C, Galvagno S, Corain B (2005) J Catal 229(2):283
16. Shahinpoor M, Kim KJ, Leo DJ (2003) Polym Compos 24(1):24
17. Shahinpoor M, Kim KJ (2002) Sens Actuators A Phys 96 (2–3):125
18. Vork FTA, Janssen LJJ, Barendrecht E (1986) Electrochim Acta 31:1569
19. Takenaka H, Torikai E, Kawami Y, Wakabayashi N (1982) Int J Hydrogen Energy 7:397
20. Millet P, Durand R, Dartyge E, Tourillon G, Fontaine A (1993) J Electrochem Soc 140:1373
21. Weppner W (1987) Sens Actuators 12:107
22. Chang SC, Stetter JR, Cha CS (1993) Talanta 40:461
23. Millet P, Pineri M, Durand R (1989) J Appl Electrochem 19:162
24. Sakthivel M, Weppner W (2005) Ionics 11:177
25. Halim J, Büchi FN, Haas O, Stamm M, Scherer GG (1994) Electrochimica Acta 39:1303
26. Langford JI (1971) Appl Cryst 4:164
27. Sakthivel M, Weppner W (2006) Sens Actuators B 113:998
28. Hwang BJ, Liu YC, Hsu WC (1998) J Solid State Electrochem 2:378
29. Frumkin AN (1963) Hydrogen overvoltage and adsorption phenomena, part II. In: Delahay P, Tobias CW (eds) Advances in electrochemistry and electrochemical engineering, vol 3. Wiley-Interscience, New York, pp 287–391
30. Paddison SJ, Paul R, Zawodzinski TA (2000) J Electrochem Soc 147:617
31. Zheng CZ, Yeung CK, Loy MMT, Xiao X (2004) Phys Rev B Condens Matter 70:205401–205402